Observation of χ_{c2}→η^{′}η^{′} and χ_{c0,2}→ηη^{′}

M. Ablikim *et al.* (BESIII Collaboration)

Phys. Rev. D **96**, 112006 — Published 18 December 2017

DOI: 10.1103/PhysRevD.96.112006

Observation of $\chi_{c2} \to \eta'\eta'$ and $\chi_{c0,2} \to \eta\eta'$

M. Ablikim[1], M. N. Achasov[9,d], S. Ahmed[14], M. Albrecht[4], A. Amoroso[53A,53C], F. F. An[1], Q. An[50,40], J. Z. Bai[1], Y. Bai[39], O. Bakina[24], R. Baldini Ferroli[20A], Y. Ban[32], D. W. Bennett[19], J. V. Bennett[5], N. Berger[23], M. Bertani[20A], D. Bettoni[21A], J. M. Bian[47], F. Bianchi[53A,53C], E. Boger[24,b], I. Boyko[24], R. A. Briere[5], H. Cai[55], X. Cai[1,40], O. Cakir[43A], A. Calcaterra[20A], G. F. Cao[1,44], S. A. Cetin[43B], J. Chai[53C], J. F. Chang[1,40], G. Chelkov[24,b,c], G. Chen[1], H. S. Chen[1,44], J. C. Chen[1], M. L. Chen[1,40], S. J. Chen[30], X. R. Chen[27], Y. B. Chen[1,40], X. K. Chu[32], G. Cibinetto[21A], H. L. Dai[1,40], J. P. Dai[35,h], A. Dbeyssi[14], D. Dedovich[24], Z. Y. Deng[1], A. Denig[23], I. Denysenko[24], M. Destefanis[53A,53C], F. De Mori[53A,53C], Y. Ding[28], C. Dong[31], J. Dong[1,40], L. Y. Dong[1,44], M. Y. Dong[1,40,44], O. Dorjkhaidav[22], Z. L. Dou[30], S. X. Du[57], P. F. Duan[1], J. Fang[1,40], S. S. Fang[1,44], X. Fang[50,40], Y. Fang[1], R. Farinelli[21A,21B], L. Fava[53B,53C], S. Fegan[23], F. Feldbauer[23], G. Felici[20A], C. Q. Feng[50,40], E. Fioravanti[21A], M. Fritsch[23,14], C. D. Fu[1], Q. Gao[1], X. L. Gao[50,40], Y. Gao[42], Y. G. Gao[6], Z. Gao[50,40], I. Garzia[21A], K. Goetzen[10], L. Gong[31], W. X. Gong[1,40], W. Gradl[23], M. Greco[53A,53C], M. H. Gu[1,40], S. Gu[15], Y. T. Gu[12], A. Q. Guo[1], L. B. Guo[29], R. P. Guo[1], Y. P. Guo[23], Z. Haddadi[26], S. Han[55], X. Q. Hao[15], F. A. Harris[45], K. L. He[1,44], X. Q. He[49], F. H. Heinsius[4], T. Held[4], Y. K. Heng[1,40,44], T. Holtmann[4], Z. L. Hou[1], C. Hu[29], H. M. Hu[1,44], T. Hu[1,40,44], Y. Hu[1], G. S. Huang[50,40], J. S. Huang[15], X. T. Huang[34], X. Z. Huang[30], Z. L. Huang[28], T. Hussain[52], W. Ikegami Andersson[54], Q. Ji[1], Q. P. Ji[15], X. B. Ji[1,44], X. L. Ji[1,40], X. S. Jiang[1,40,44], X. Y. Jiang[31], J. B. Jiao[34], Z. Jiao[17], D. P. Jin[1,40,44], S. Jin[1,44], Y. Jin[46], T. Johansson[54], A. Julin[47], N. Kalantar-Nayestanaki[26], X. L. Kang[1], X. S. Kang[31], M. Kavatsyuk[26], B. C. Ke[5], T. Khan[50,40], A. Khoukaz[48], P. Kiese[23], R. Kliemt[10], L. Koch[25], O. B. Kolcu[43B,f], B. Kopf[4], M. Kornicer[45], M. Kuemmel[4], M. Kuhlmann[4], A. Kupsc[54], W. Kühn[25], J. S. Lange[25], M. Lara[19], P. Larin[14], L. Lavezzi[53C], H. Leithoff[23], C. Leng[53C], C. Li[54], Cheng Li[50,40], D. M. Li[57], F. Li[1,40], F. Y. Li[32], G. Li[1], H. B. Li[1,44], H. J. Li[1], J. C. Li[1], Jin Li[33], K. J. Li[41], Kang Li[13], Ke Li[34], Lei Li[3], P. L. Li[50,40], P. R. Li[44,7], Q. Y. Li[34], T. Li[34], W. D. Li[1,44], W. G. Li[1], X. L. Li[34], X. N. Li[1,40], X. Q. Li[31], Z. B. Li[41], H. Liang[50,40], Y. F. Liang[37], Y. T. Liang[25], G. R. Liao[11], D. X. Lin[14], B. Liu[35,h], B. J. Liu[1], C. X. Liu[1], D. Liu[50,40], F. H. Liu[36], Fang Liu[1], Feng Liu[6], H. B. Liu[12], H. M. Liu[1,44], Huanhuan Liu[1], Huihui Liu[16], J. B. Liu[50,40], J. P. Liu[55], J. Y. Liu[1], K. Liu[42], K. Y. Liu[28], Ke Liu[6], L. D. Liu[32], P. L. Liu[1,40], Q. Liu[44], S. B. Liu[50,40], X. Liu[27], Y. B. Liu[31], Z. A. Liu[1,40,44], Zhiqing Liu[23], Y. F. Long[32], X. C. Lou[1,40,44], H. J. Lu[17], J. G. Lu[1,40], Y. Lu[1], Y. P. Lu[1,40], C. L. Luo[29], M. X. Luo[56], X. L. Luo[1,40], X. R. Lyu[44], F. C. Ma[28], H. L. Ma[1], L. L. Ma[34], M. M. Ma[1], Q. M. Ma[1], T. Ma[1], X. N. Ma[31], X. Y. Ma[1,40], Y. M. Ma[34], F. E. Maas[14], M. Maggiora[53A,53C], Q. A. Malik[52], Y. J. Mao[32], Z. P. Mao[1], S. Marcello[53A,53C], Z. X. Meng[46], J. G. Messchendorp[26], G. Mezzadri[21B], J. Min[1,40], T. J. Min[1], R. E. Mitchell[19], X. H. Mo[1,40,44], Y. J. Mo[6], C. Morales Morales[14], G. Morello[20A], N. Yu. Muchnoi[9,d], H. Muramatsu[47], P. Musiol[4], A. Mustafa[4], Y. Nefedov[24], F. Nerling[10], I. B. Nikolaev[9,d], Z. Ning[1,40], S. Nisar[8], S. L. Niu[1,40], X. Y. Niu[1], S. L. Olsen[33], Q. Ouyang[1,40,44], S. Pacetti[20B], Y. Pan[50,40], M. Papenbrock[54], P. Patteri[20A], M. Pelizaeus[4], J. Pellegrino[53A,53C], H. P. Peng[50,40], K. Peters[10,g], J. Pettersson[54], J. L. Ping[29], R. G. Ping[1,44], A. Pitka[23], R. Poling[47], V. Prasad[50,40], H. R. Qi[2], M. Qi[30], S. Qian[1,40], C. F. Qiao[44], J. J. Qin[44], N. Qin[55], X. S. Qin[4], Z. H. Qin[1,40], J. F. Qiu[1], K. H. Rashid[52,i], C. F. Redmer[23], M. Richter[4], M. Ripka[23], M. Rolo[53C], G. Rong[1,44], Ch. Rosner[14], X. D. Ruan[12], A. Sarantsev[24,e], M. Savrié[21B], C. Schnier[4], K. Schoenning[54], W. Shan[32], M. Shao[50,40], C. P. Shen[2], P. X. Shen[31], X. Y. Shen[1,44], H. Y. Sheng[1], J. J. Song[34], W. M. Song[34], X. Y. Song[1], S. Sosio[53A,53C], C. Sowa[4], S. Spataro[53A,53C], G. X. Sun[1], J. F. Sun[15], L. Sun[55], S. S. Sun[1,44], X. H. Sun[1], Y. J. Sun[50,40], Y. K Sun[50,40], Y. Z. Sun[1], Z. J. Sun[1,40], Z. T. Sun[19], C. J. Tang[37], G. Y. Tang[1], X. Tang[1], I. Tapan[43C], M. Tiemens[26], B. T. Tsednee[22], I. Uman[43D], G. S. Varner[45], B. Wang[1], B. L. Wang[44], D. Wang[32], D. Y. Wang[32], Dan Wang[44], K. Wang[1,40], L. L. Wang[1], L. S. Wang[1], M. Wang[34], P. Wang[1], P. L. Wang[1], W. P. Wang[50,40], X. F. Wang[42], Y. Wang[38], Y. D. Wang[14], Y. F. Wang[1,40,44], Y. Q. Wang[23], Z. Wang[1,40], Z. G. Wang[1,40], Z. H. Wang[50,40], Z. Y. Wang[1], Zongyuan Wang[1], T. Weber[23], D. H. Wei[11], J. H. Wei[31], P. Weidenkaff[23], S. P. Wen[1], U. Wiedner[4], M. Wolke[54], L. H. Wu[1], L. J. Wu[1], Z. Wu[1,40], L. Xia[50,40], Y. Xia[18], D. Xiao[1], H. Xiao[51], Y. J. Xiao[1], Z. J. Xiao[29], Y. G. Xie[1,40], Y. H. Xie[6], X. A. Xiong[1], Q. L. Xiu[1,40], G. F. Xu[1], J. J. Xu[1], L. Xu[1], Q. J. Xu[13], Q. N. Xu[44], X. P. Xu[38], L. Yan[53A,53C], W. B. Yan[50,40], W. C. Yan[50,40], Y. H. Yan[18], H. J. Yang[35,h], H. X. Yang[1], L. Yang[55], Y. H. Yang[30], Y. X. Yang[11], M. Ye[1,40], M. H. Ye[7], J. H. Yin[1], Z. Y. You[41], B. X. Yu[1,40,44], C. X. Yu[31], J. S. Yu[27], C. Z. Yuan[1,44], Y. Yuan[1], A. Yuncu[43B,a], A. A. Zafar[52], Y. Zeng[18], Z. Zeng[50,40], B. X. Zhang[1], B. Y. Zhang[1,40], C. C. Zhang[1], D. H. Zhang[1], H. H. Zhang[41], H. Y. Zhang[1,40], J. Zhang[1], J. L. Zhang[1], J. Q. Zhang[1], J. W. Zhang[1,40,44], J. Y. Zhang[1], J. Z. Zhang[1,44], K. Zhang[1], L. Zhang[42], S. Q. Zhang[31], X. Y. Zhang[34], Y. H. Zhang[1,40], Y. T. Zhang[50,40], Yang Zhang[1], Yao Zhang[1], Yu Zhang[44], Z. H. Zhang[6], Z. P. Zhang[50], Z. Y. Zhang[55], G. Zhao[1], J. W. Zhao[1,40], J. Y. Zhao[1], J. Z. Zhao[1,40], Lei Zhao[50,40], Ling Zhao[1], M. G. Zhao[31], Q. Zhao[1], S. J. Zhao[57], T. C. Zhao[1], Y. B. Zhao[1,40], Z. G. Zhao[50,40], A. Zhemchugov[24,b], B. Zheng[51,14], J. P. Zheng[1,40], W. J. Zheng[34], Y. H. Zheng[44], B. Zhong[29], L. Zhou[1,40], X. Zhou[55], X. K. Zhou[50,40], X. R. Zhou[50,40], X. Y. Zhou[1], Y. X. Zhou[12], J. Zhu[41], K. Zhu[1], K. J. Zhu[1,40,44], S. Zhu[1], S. H. Zhu[49], X. L. Zhu[42], Y. C. Zhu[50,40], Y. S. Zhu[1,44], Z. A. Zhu[1,44], J. Zhuang[1,40], L. Zotti[53A,53C], B. S. Zou[1], J. H. Zou[1]

(BESIII Collaboration)

[1] *Institute of High Energy Physics, Beijing 100049, People's Republic of China*
[2] *Beihang University, Beijing 100191, People's Republic of China*
[3] *Beijing Institute of Petrochemical Technology, Beijing 102617, People's Republic of China*
[4] *Bochum Ruhr-University, D-44780 Bochum, Germany*
[5] *Carnegie Mellon University, Pittsburgh, Pennsylvania 15213, USA*
[6] *Central China Normal University, Wuhan 430079, People's Republic of China*
[7] *China Center of Advanced Science and Technology, Beijing 100190, People's Republic of China*
[8] *COMSATS Institute of Information Technology, Lahore, Defence Road, Off Raiwind Road, 54000 Lahore, Pakistan*

[9] G.I. Budker Institute of Nuclear Physics SB RAS (BINP), Novosibirsk 630090, Russia
[10] GSI Helmholtzcentre for Heavy Ion Research GmbH, D-64291 Darmstadt, Germany
[11] Guangxi Normal University, Guilin 541004, People's Republic of China
[12] Guangxi University, Nanning 530004, People's Republic of China
[13] Hangzhou Normal University, Hangzhou 310036, People's Republic of China
[14] Helmholtz Institute Mainz, Johann-Joachim-Becher-Weg 45, D-55099 Mainz, Germany
[15] Henan Normal University, Xinxiang 453007, People's Republic of China
[16] Henan University of Science and Technology, Luoyang 471003, People's Republic of China
[17] Huangshan College, Huangshan 245000, People's Republic of China
[18] Hunan University, Changsha 410082, People's Republic of China
[19] Indiana University, Bloomington, Indiana 47405, USA
[20] (A)INFN Laboratori Nazionali di Frascati, I-00044, Frascati, Italy; (B)INFN and University of Perugia, I-06100, Perugia, Italy
[21] (A)INFN Sezione di Ferrara, I-44122, Ferrara, Italy; (B)University of Ferrara, I-44122, Ferrara, Italy
[22] Institute of Physics and Technology, Peace Ave. 54B, Ulaanbaatar 13330, Mongolia
[23] Johannes Gutenberg University of Mainz, Johann-Joachim-Becher-Weg 45, D-55099 Mainz, Germany
[24] Joint Institute for Nuclear Research, 141980 Dubna, Moscow region, Russia
[25] Justus-Liebig-Universitaet Giessen, II. Physikalisches Institut, Heinrich-Buff-Ring 16, D-35392 Giessen, Germany
[26] KVI-CART, University of Groningen, NL-9747 AA Groningen, The Netherlands
[27] Lanzhou University, Lanzhou 730000, People's Republic of China
[28] Liaoning University, Shenyang 110036, People's Republic of China
[29] Nanjing Normal University, Nanjing 210023, People's Republic of China
[30] Nanjing University, Nanjing 210093, People's Republic of China
[31] Nankai University, Tianjin 300071, People's Republic of China
[32] Peking University, Beijing 100871, People's Republic of China
[33] Seoul National University, Seoul, 151-747 Korea
[34] Shandong University, Jinan 250100, People's Republic of China
[35] Shanghai Jiao Tong University, Shanghai 200240, People's Republic of China
[36] Shanxi University, Taiyuan 030006, People's Republic of China
[37] Sichuan University, Chengdu 610064, People's Republic of China
[38] Soochow University, Suzhou 215006, People's Republic of China
[39] Southeast University, Nanjing 211100, People's Republic of China
[40] State Key Laboratory of Particle Detection and Electronics, Beijing 100049, Hefei 230026, People's Republic of China
[41] Sun Yat-Sen University, Guangzhou 510275, People's Republic of China
[42] Tsinghua University, Beijing 100084, People's Republic of China
[43] (A)Ankara University, 06100 Tandogan, Ankara, Turkey; (B)Istanbul Bilgi University, 34060 Eyup, Istanbul, Turkey; (C)Uludag University, 16059 Bursa, Turkey; (D)Near East University, Nicosia, North Cyprus, Mersin 10, Turkey
[44] University of Chinese Academy of Sciences, Beijing 100049, People's Republic of China
[45] University of Hawaii, Honolulu, Hawaii 96822, USA
[46] University of Jinan, Jinan 250022, People's Republic of China
[47] University of Minnesota, Minneapolis, Minnesota 55455, USA
[48] University of Muenster, Wilhelm-Klemm-Str. 9, 48149 Muenster, Germany
[49] University of Science and Technology Liaoning, Anshan 114051, People's Republic of China
[50] University of Science and Technology of China, Hefei 230026, People's Republic of China
[51] University of South China, Hengyang 421001, People's Republic of China
[52] University of the Punjab, Lahore-54590, Pakistan
[53] (A)University of Turin, I-10125, Turin, Italy; (B)University of Eastern Piedmont, I-15121, Alessandria, Italy; (C)INFN, I-10125, Turin, Italy
[54] Uppsala University, Box 516, SE-75120 Uppsala, Sweden
[55] Wuhan University, Wuhan 430072, People's Republic of China
[56] Zhejiang University, Hangzhou 310027, People's Republic of China
[57] Zhengzhou University, Zhengzhou 450001, People's Republic of China

[a] Also at Bogazici University, 34342 Istanbul, Turkey
[b] Also at the Moscow Institute of Physics and Technology, Moscow 141700, Russia
[c] Also at the Functional Electronics Laboratory, Tomsk State University, Tomsk, 634050, Russia
[d] Also at the Novosibirsk State University, Novosibirsk, 630090, Russia
[e] Also at the NRC "Kurchatov Institute", PNPI, 188300, Gatchina, Russia
[f] Also at Istanbul Arel University, 34295 Istanbul, Turkey
[g] Also at Goethe University Frankfurt, 60323 Frankfurt am Main, Germany
[h] Also at Key Laboratory for Particle Physics, Astrophysics and Cosmology, Ministry of Education; Shanghai Key Laboratory for Particle Physics and Cosmology; Institute of Nuclear and Particle Physics, Shanghai 200240, People's Republic of China
[i] Government College Women University, Sialkot - 51310. Punjab, Pakistan.

Using a sample of 448.1×10^6 $\psi(3686)$ events collected with the BESIII detector in 2009 and 2012, we study the decays $\chi_{c0,2}\to\eta'\eta'$ and $\eta\eta'$. The decays $\chi_{c2}\to\eta'\eta'$, $\chi_{c0}\to\eta\eta'$ and $\chi_{c2}\to\eta\eta'$ are observed for the first time with statistical significances of 9.6σ, 13.4σ and 7.5σ, respectively. The branching fractions are determined to be $\mathcal{B}(\chi_{c0}\to\eta'\eta')=(2.19\pm0.03\pm0.14)\times10^{-3}$, $\mathcal{B}(\chi_{c2}\to\eta'\eta')=(4.76\pm0.56\pm0.38)\times10^{-5}$, $\mathcal{B}(\chi_{c0}\to\eta\eta')=(8.92\pm0.84\pm0.65)\times10^{-5}$ and $\mathcal{B}(\chi_{c2}\to\eta\eta')=(2.27\pm0.43\pm0.25)\times10^{-5}$, where the first uncertainties are statistical and the second are systematic. The precision for the measurement of $\mathcal{B}(\chi_{c0}\to\eta'\eta')$ is significantly improved compared to previous measurements. Based on the measured branching fractions, the role played by the doubly and singly Okubo-Zweig-Iizuka disconnected transition amplitudes for $\chi_{c0,2}$ decays into pseudoscalar meson pairs can be clarified.

PACS numbers: 13.25.Gv

I. INTRODUCTION

During the past decades an enormous number of decay channels have been measured for J/ψ and $\psi(3686)$ [Note*]. It can be attributed to the accumulation of high statistics of J/ψ and $\psi(3686)$ events which can be accessed directly in e^+e^- annihilations. As a result, many interesting properties associated with the strong decays of J/ψ and $\psi(3686)$ have been investigated and will advance our knowledge about the strong QCD in the interplay of perturbative and non-perturbative strong interaction regime. In contrast, little is known about the χ_{cJ} ($J=0,\ 1,\ 2$) decays since they can not be produced directly in e^+e^- annihilation due to spin-parity conservation. In Ref. [1] it was argued that the ratio of the decay branching fractions between $J/\psi\to\omega f_0(1710)$ and $J/\psi\to\phi f_0(1710)$ [2] encodes the production mechanisms of light quark contents via the Okubo-Zweig-Iizuka (OZI) rule violations. In Refs. [3, 4] parametrization schemes were proposed in order to further understand the OZI rule violating mechanisms in the two-body decays of χ_{cJ} to SS, PP and VV ($S=$ scalar, $P=$ pseudoscalar, $V=$ vector). It was shown that apart from the singly OZI (SOZI) disconnected process, the doubly OZI (DOZI) disconnected process may play a crucial role in the production of isospin-0 light meson pairs, for instance, in $\chi_{cJ}\to f_0f_0'$, $\omega\omega$, $\phi\phi$, $\omega\phi$, $\eta\eta$, $\eta\eta'$ and $\eta'\eta'$. By defining the relative strength r between the DOZI and SOZI violating amplitudes in addition to several other physical quantities in the SU(3) flavor basis, insights into the mechanisms for producing light meson pairs in charmonium decays can be gained.

Several $\chi_{c0}\to SS$ decay processes have been previously observed and measured [5], but no definitive conclusions can yet be drawn. In the $\chi_{cJ}\to VV$ sector, BESIII's results [6] indicate that violation of the OZI rule and SU(3) flavor symmetry breaking are significant in $\chi_{c0}\to VV$ decays, but small in $\chi_{c2}\to VV$ decays [3]. Furthermore, the observation of a small $\chi_{c0}\to\omega\phi$ branching fraction and upper limits on $\chi_{c2}\to\omega\phi$ imply a small DOZI contribution in $\chi_{c0,2}\to VV$ decays. As for $\chi_{c0,2}\to PP$ decays, most of them have been well measured except for the processes with final states containing an η' meson. Until now, only the branching fraction of $\chi_{c0}\to\eta'\eta'$ is available with poor precision, while no obvious signals for $\chi_{c2}\to\eta'\eta'$ and $\chi_{c0,2}\to\eta\eta'$ are observed [2]. It is worth noting that according to Eq. 15 in Ref. [3] the calculation of r is more sensitive to the branching fractions of $\chi_{c0,2}\to\eta'\eta'$ and $\eta\eta'$ than those of $\chi_{c0,2}\to\eta\eta$ [3, 4]. Therefore, measurements of $\chi_{c0,2}\to\eta'\eta'$ and $\eta\eta'$ are desirable and crucial to disentangle the roles played by OZI violation in charmonium decay.

In this article, we report measurements of the branching fractions of $\chi_{c0,2}\to\eta'\eta'$ and $\eta\eta'$ based on a data sample of 448.1×10^6 $\psi(3686)$ events [7, 8] collected with the BESIII detector [9] operated at the BEPCII storage ring in 2009 and 2012. The number of $\psi(3686)$ events, determined by measuring inclusive hadronic events, is $(107.0\pm0.8)\times10^6$ for 2009 and $(341.1\pm2.1)\times10^6$ for 2012.

II. THE BESIII DETECTOR AND SIMULATION

The BESIII detector is composed of four sub-detectors: the main drift chamber (MDC), the time-of-flight counter (TOF), the electromagnetic calorimeter (EMC) and the muon counter (MUC). There is a superconducting solenoid magnet surrounding the electromagnetic calorimeter, providing a 1 Tesla (0.9 Tesla during 2012 data taking) magnetic field. The details of the BESIII detector can be found in Ref. [9]. The BESIII detector is simulated by the GEANT4-based [10] simulation software BOOST [11], which includes the geometric and material description of the BESIII detector, the detector response and digitization models, as well as a record of the detector running conditions and performances. The production of the $\psi(3686)$ resonance is simulated by the Monte Carlo (MC) generator KKMC [12], in which the effects of beam energy spread and initial state radiation are considered. Known decays are generated by EVTGEN [13] using branching fractions quoted by the particle data group (PDG) [2], and the remaining un-

Note* $\psi(3686)$ denotes the state called $\psi(2S)$ by PDG.

known decays are generated with LUNDCHARM [14]. The transition of $\psi(3686) \to \gamma\chi_{cJ}$ is assumed to be a pure $E1$ process [15]. The subsequent decay $\chi_{c0} \to \eta'\eta'/\eta\eta'$ with η and η' decay to the specific final states listed in the following paragraph are generated by assuming a uniform phase space distribution, while the angular distributions of η and η' in χ_{c2} decays are taken as those of $\pi^{\pm}$ in Ref. [16], which is the measurement with the highest precision until now.

To increase statistics, two dominant η' decay modes, $\eta' \to \gamma\pi^+\pi^-$ and $\eta' \to \eta\pi^+\pi^-$, are considered, while the η is reconstructed in its prominent decay mode $\eta \to \gamma\gamma$. Consequently, there are three decay modes in the study of $\chi_{c0,2} \to \eta'\eta'$: both η' decay to $\gamma\pi^+\pi^-$ (mode A), both η' decay to $\eta\pi^+\pi^-$ (mode B), and one η' decays to $\gamma\pi^+\pi^-$ while the other η' decays to $\eta\pi^+\pi^-$ (mode C). Two decay modes are considered for $\chi_{c0,2} \to \eta\eta'$: η' decays to $\gamma\pi^+\pi^-$ (mode I) and to $\eta\pi^+\pi^-$ (mode II).

III. EVENT SELECTION

Charged tracks are reconstructed using MDC hits within the acceptance range of $|\cos\theta| < 0.93$, where θ is the polar angle with respect to the electron beam direction. They are required to originate from the interaction region, defined as $R_{xy} < 1$ cm and $|V_z| < 10$ cm, where R_{xy} and $|V_z|$ are the distances of closest approach in the xy-plane and the z direction, respectively. All charged tracks are assumed to be pions. The candidate photons are selected using EMC showers. The photon energy deposited in the EMC is required to be larger than 25 MeV in the barrel region ($|\cos\theta| < 0.8$) or 50 MeV in the end caps region ($0.86 < |\cos\theta| < 0.92$). The EMC hit time of the photon candidate must be within the range $0 \le t \le 700$ ns from the event start time to suppress electronic noise and energy deposits unrelated to the event. An η candidate is reconstructed from a pair of photons with an invariant mass $M_{\gamma\gamma}$ satisfying $|M_{\gamma\gamma} - M_\eta| < 20$ MeV/c^2, where M_η is the nominal η mass [2].

A four momentum constrained kinematic fit to the initial beam four momentum, with an additional mass constraint on η candidates, is imposed on the candidate charged tracks and photons with the proper charged tracks and photons hypothesis, to improve the mass resolution and suppress backgrounds. If additional photons are found in an event, the combination of photons with the least χ^2 is retained for further analysis. The resulting χ^2 of the kinematic fit is required to be less than a decay mode dependent value, ranging from 25 to 90, which is obtained by optimizing the figure-of-merit $N_S^{\rm MC}/\sqrt{N_S^{\rm data} + N_B^{\rm data}}$, where $N_S^{\rm MC}$ is the number of events from the signal MC sample, and $N_S^{\rm data}$ and $N_B^{\rm data}$ represent the numbers of signal and background events from data, respectively.

An inclusive MC sample containing 3.64×10^8 $\psi(3686)$ events and 48 pb^{-1} of data collected at center-of-mass energy $\sqrt{s} = 3.65$ GeV [17], which is about one fifteenth of the integrated luminosity of the $\psi(3686)$ data, are employed to investigate the potential backgrounds. Studies of the MC sample indicate the common backgrounds for all decay modes are from $\psi(3686) \to \pi^0 + X$ (X represents all possible final states) and $\psi(3686) \to \pi^+\pi^- J/\psi$ decays. The former one is suppressed by requiring the invariant mass of any two photons $M_{\gamma\gamma}$ to be out of the π^0 mass region, $|M_{\gamma\gamma} - M_{\pi^0}| > 15$ MeV/c^2, where M_{π^0} is the nominal π^0 mass [2]. The latter one is suppressed by requiring the recoil mass of any $\pi^+\pi^-$ combination $M^{\rm rec}_{\pi^+\pi^-}$ to be out of the J/ψ mass region $|M^{\rm rec}_{\pi^+\pi^-} - M_{J/\psi}| > 5$ MeV/c^2, where $M_{J/\psi}$ is the nominal J/ψ mass [2]. For the $\chi_{c0,2} \to \eta\eta'$ channel, there is background from $\chi_{c0,2} \to \gamma J/\psi, J/\psi \to \gamma\eta'$, which is suppressed by further requiring the invariant mass of any $\gamma\eta'$ combination to be out of the region (3.05, 3.16) GeV/c^2 for mode I and (3.049, 3.199) GeV/c^2 for mode II, respectively, where the γ is from the η candidates. The cross contaminations between different decay modes are studied and are found to be negligible. For the data at $\sqrt{s} = 3.65$ GeV, there are almost no events satisfying the above selection criteria, which indicates that the background due to continuum production is negligible.

For the $\chi_{c0,2} \to \eta'\eta'$ decay, the two η' candidates are selected by minimizing $(M_i - M_{\eta'})^2 + (M_j - M_{\eta'})^2$. Here, the subscripts $i/j = 1$ or 2 denote $\gamma\pi^+\pi^-$ or $\eta\pi^+\pi^-$ for the two different decay modes, respectively, and $M_{\eta'}$ is the η' nominal mass [2]. Figures 1(a), (b) and (c) show the scatter plots of M_i versus M_j of the candidate events for the modes A, B, and C individually. The double-η' signal region is defined as $M_1 \in (0.943, 0.973)$ GeV/c^2 for mode A, $M_2 \in (0.928, 0.988)$ GeV/c^2 for mode B, and $M_1 \in (0.933, 0.983)$ GeV/c^2 and $M_2 \in (0.943, 0.973)$ GeV/c^2 for mode C. Clear double-η' signals are seen in the intersection region (shown as the central square) for each mode. The eight squares with equal area around the signal region are selected to be sideband regions, which are classified into two categories: the four boxes in the corners are used to estimate the background contribution from background without η' in subsequent decays (namely type A), and the remaining four boxes are used to estimate the background with one η' in subsequent decays (namely type B).

For the $\chi_{c0,2} \to \eta\eta'$ decay, the η' candidate is selected if it has a minimum $|M_i - M_{\eta'}|$. Figure 2 shows the M_i distributions of the candidate events for the two η' decay modes, where clear η' signals are observed in both modes. The η' signal region is defined as $M_1 \in (0.948, 0.968)$ GeV/c^2 or $M_2 \in (0.943, 0.973)$ GeV/c^2, and two sideband regions with width equal to that of the signal region are chosen around the signal region for each decay mode.

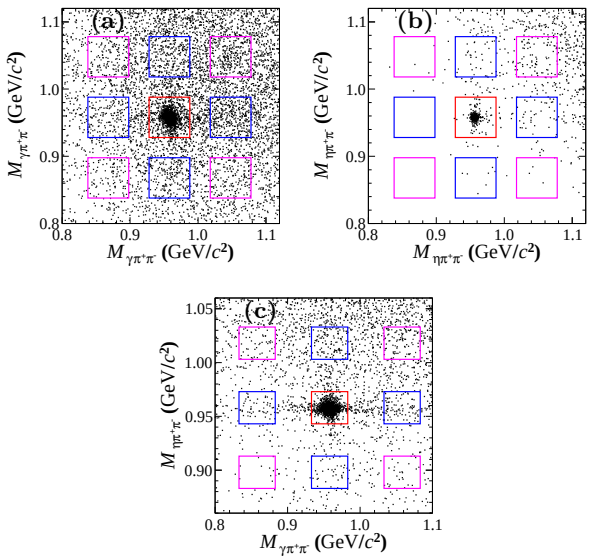

Figure 1. Scatter plots of M_i versus M_j of the candidate events for modes (a) A, (b) B, and (c) C from the $\psi(3686)$ data. The boxes denote the signal and background regions described in the text.

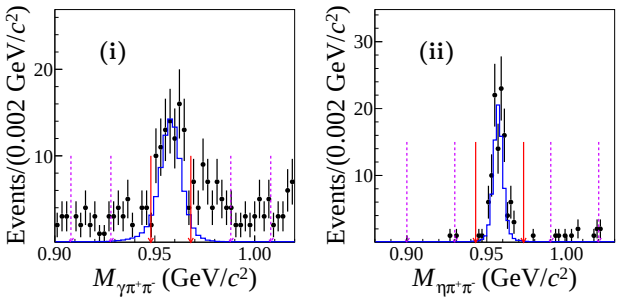

Figure 2. The M_i distributions of the η' candidate events for modes (i) I and (ii) II. In each plot, the dots with error bars are for the $\psi(3686)$ data, and the histograms are for the signal MC samples, the solid arrows show the η' signal regions and the dashed ones show sideband regions.

IV. DATA ANALYSIS

Figure 3(a)-(c) shows the spectra of $\eta'\eta'$ invariant mass $M_{\eta'\eta'}$ for the candidate events in the modes A, B, and C, respectively, while Fig. 3(d) shows the corresponding distribution summed over the three decay modes. Clear $\chi_{c0,2}$ signals are observed. The expected background, which is estimated with the events within the sideband regions normalized by $\frac{1}{2}M^{\rm B}_{\rm side} - \frac{1}{4}M^{\rm A}_{\rm side}$, are presented as histograms in the corresponding figures, where $M^{\rm A}_{\rm side}$ and $M^{\rm B}_{\rm side}$ are the corresponding distributions in the sidebands A and B regions, and we assume the background is distributed uniformly around the η' signal region. No obvious $\chi_{c0,2}$ peaks are found in the sideband regions, while χ_{c1} peaks are seen in modes A and C. A study with the inclusive MC sample indicates that the small bump around the χ_{c1} mass region for mode A comes from the $\chi_{c1} \to \gamma J/\psi$, $J/\psi \to \gamma 2(\pi^+\pi^-)$ channel, while that for mode C comes from $\chi_{c1} \to f_0(980)\eta'$, which will be considered later.

Figures 3(i) and (ii) show the distributions of $\eta\eta'$ invariant mass $M_{\eta\eta'}$ for the two η' decay modes, where clear $\chi_{c0,2}$ signals are visible. The normalized events in the η' sideband region are also depicted and no obvious $\chi_{c0,2}$ peaks are observed, while the χ_{c1} signal is seen in mode I. Analysis with an inclusive MC sample indicates that the small χ_{c1} bump in mode I comes from the processes $\psi(3686) \to \gamma\chi_{c1}$, $\chi_{c1} \to \gamma J/\psi$, $J/\psi \to \gamma\gamma\pi^+\pi^-(\eta\pi^+\pi^-$ or $\gamma\eta'$ with $\eta' \to \gamma\pi^+\pi^-$, etc.), which will be taken into account in the fit later.

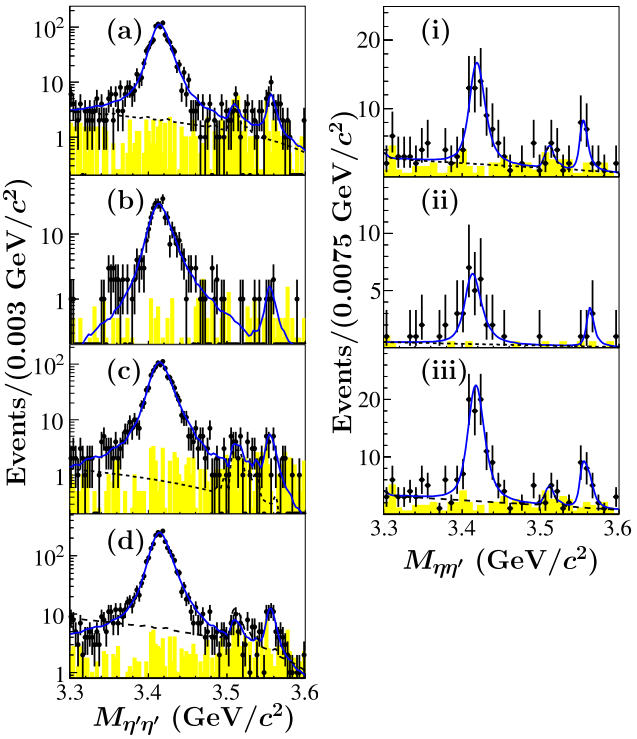

Figure 3. Left column shows the simultaneous fits for $\chi_{c0,2} \to \eta'\eta'$. (a) Mode A. (b) Mode B. (c) Mode C. (d) Sum of (a), (b), and (c). Right column shows the simultaneous fits for $\chi_{c0,2} \to \eta\eta'$. (i) Mode I. (ii) Mode II. (iii) Sum of (i) and (ii). In all of the above plots, the dots with error bars denote the $\psi(3686)$ data, the solid line denotes the overall fit results, the dashed line denotes the backgrounds and the yellow histogram shows the normalized events in the η' sideband regions.

To determine the branching fractions of $\chi_{c0,2} \to \eta'\eta'$ and $\eta\eta'$, two simultaneous fits to the three $M_{\eta'\eta'}$ spectra and the two $M_{\eta\eta'}$ spectra are performed. The overall probability density functions in fitting include three components: the $\chi_{c0,2}$ signals, the χ_{c1} peaking background for specific modes, and the non-peaking background. In the fit, the $\chi_{c0,2}$ signals are described with

the MC-simulated shape of histogram convolved with a Gaussian function to compensate for the potential resolution difference between data and MC simulation. Due to limited-size of data sample, the parameters of the Gaussian function are fixed to those obtained from control samples, such as $\psi(3686) \to \gamma\chi_{c0,2}$ with $\chi_{c0,2} \to 2(\pi^+\pi^-)$, $\psi(3686) \to \gamma\chi_{c0,2}$ with $\chi_{c0,2} \to 2(\pi^+\pi^-\pi^0)$, which have similar final states of interest. The shape of the χ_{c1} peaking background for the specific modes are described with the MC simulation of the corresponding background modes, and their magnitudes are floated. The non-peaking backgrounds are described by a first order Chebychev polynomial. In the fit, the branching fractions of $\chi_{c0,2} \to \eta'\eta'/\eta\eta'$, $\mathcal{B}(\chi_{c0,2} \to \eta'\eta'/\eta\eta')$, are taken as the common parameters among the different decay modes. The projections of the simultaneous fit are shown in Fig. 3. The statistical significance are 9.6σ for $\chi_{c2} \to \eta'\eta'$, 13.4σ for $\chi_{c0} \to \eta\eta'$ and 7.5σ for $\chi_{c2} \to \eta\eta'$, individually, which are determined by comparing the fit likelihood values with and without the corresponding $\chi_{c0,2}$ signal included. The detection efficiencies ϵ, the $\chi_{c0,2}$ signal yields in the different decay modes, and the resultant decay branching fractions are summarized in Table I, where the signal yields in each decay mode are calculated according to the total number $N_{\psi(3686)}$ of $\psi(3686)$ events, the detection efficiency and the product branching fractions in the subsequent decay. For mode C, there is a factor of two to account for the identical particles. Except for the $\mathcal{B}(\chi_{c0,2} \to \eta'\eta'/\eta\eta')$ obtained in this measurement, all other decay branching fractions are taken from the PDG [2]. The fitted numbers of χ_{c1} background are found to be consistent with the expectations from the MC simulation.

V. SYSTEMATIC UNCERTAINTY

Several sources of systematic uncertainty in the branching fraction measurements are considered. The systematic uncertainty from the total number of $\psi(3686)$ events, estimated by measuring inclusive hadronic events, is 0.7% [7, 8]. The uncertainty from MDC tracking and photon detection have been studied with the high purity control sample of $\psi(3686) \to \pi^+\pi^- J/\psi$, $J/\psi \to l^+l^-$ and $J/\psi \to \rho\pi$. The difference in the detection efficiency between data and MC simulation is less than 1% per charged track, which is taken as the systematic uncertainty [7]. Employing a method similar to that in Ref. [18], except using a larger J/ψ data set [19], the difference of the photon detection efficiency between data and MC simulation is determined to be within 0.5% in the barrel and 1.5% in the endcaps of the EMC. In this analysis, the weighted uncertainty is 0.6% per photon by considering the photon angular distribution. The uncertainty due to η reconstruction is determined by using a high purity control sample of $J/\psi \to \eta p\bar{p}$ decays. The difference of η reconstruction efficiencies between data and MC simulation, about 1.0% per η [20], is taken as the systematic uncertainty. The uncertainty from the η' mass window requirement is estimated by changing the η' signal windows by one unit of the mass resolution. The resultant difference in the branching fractions is taken as the systematic uncertainty. The uncertainty related to the kinematic fit is due to the inconsistency between data and MC simulation of the track parameters and their error matrices. In this work, only charged pions are involved and their track parameters in MC simulation are corrected by using the control sample $\psi(3686) \to \pi^+\pi^- K^+K^-$. As a consequence, the consistency between data and MC simulation is significantly improved. The difference of the detection efficiencies with and without the correction is taken as the uncertainty due to the kinematic fit. The detailed method to estimate the uncertainty of the kinematic fit can be found in Ref. [21]. The uncertainty in the fit arises from resolution compensation, fit range and background shape. The resolution compensation uncertainty is obtained by changing the width of Gaussian function to the most conservative value estimated by the different control samples. The uncertainties from fit range and background shape are estimated by shifting up or down the fit intervals by 10 MeV/c^2 and by changing the order of the Chebychev polynomial function, respectively. Summing the maximum uncertainties of each aspect in quadrature yields the uncertainty from the fit. The uncertainty from decay branching fractions of intermediate states in the subsequent decays is determined by setting the branching fractions, $\mathcal{B}(\psi(3686) \to \gamma\chi_{cJ})$, $\mathcal{B}(\eta' \to \gamma\pi^+\pi^-)$, $\mathcal{B}(\eta' \to \eta\pi^+\pi^-)$, and $\mathcal{B}(\eta \to \gamma\gamma)$, randomly according to the Gaussian distributions, where the means and standard deviations of Gaussian functions are taken to be their central values of the branching fractions and the corresponding uncertainties in the PDG [2]. We repeat the same fitting process 100 times, and the standard deviations of the resultant branching fractions are taken as the systematic uncertainty. The uncertainty arising from the $\psi(3686) \to \pi^0 + X$ background subtraction is estimated by changing the π^0 mass window $|M_{\gamma\gamma} - M_{\pi^0}|$ by ± 1 MeV/c^2 in the event selection. Similarly, the uncertainty related to $\psi(3686) \to \pi^+\pi^- J/\psi$ is estimated by changing the J/ψ mass window $|M^{\rm recoil}_{\pi^+\pi^-} - M_{J/\psi}|$ by 1 MeV/c^2. The uncertainty arising from the veto $\chi_{c0,2} \to \gamma J/\psi$ with $J/\psi \to \gamma\eta'$ is estimated by shifting the J/ψ mass window by ± 1 MeV/c^2.

Table II summarizes all the systematic uncertainties for $\chi_{c0,2} \to \eta'\eta'$ and $\chi_{c0,2} \to \eta\eta'$, in which the uncertainties from photon efficiency, η reconstruction, kinematic fit, and background veto are decay mode dependent, and the weighted average uncertainties are presented. The weights are the product of the detection efficiency and the branching fractions of η' and η subsequent decays in individual decay modes. The total systematic uncertainty is obtained by adding all individual values in quadrature.

Table I. The results for $\chi_{c0,2} \to \eta'\eta'/\eta\eta'$. $\mathcal{B}$ denotes branching fraction.

Decay channel	$\chi_{c0} \to \eta'\eta'$			$\chi_{c2} \to \eta'\eta'$			$\chi_{c0} \to \eta\eta'$		$\chi_{c2} \to \eta\eta'$	
η' decay mode	Mode A	Mode B	Mode C	Mode A	Mode B	Mode C	Mode I	Mode II	Mode I	Mode II
Efficiency(%)	12.9 ± 0.1	11.9 ± 0.1	13.0 ± 0.1	14.0 ± 0.1	14.8 ± 0.1	14.9 ± 0.1	12.7 ± 0.1	9.0 ± 0.1	14.7 ± 0.1	10.4 ± 0.1
Signal number	1057 ± 15	329 ± 5	1238 ± 17	22.7 ± 2.6	8.1 ± 0.9	28.1 ± 3.3	59.9 ± 5.3	24.1 ± 2.1	14.3 ± 2.8	5.5 ± 1.1
$\mathcal{B}$ (This work)	$(2.19 \pm 0.03 \pm 0.14) \times 10^{-3}$			$(4.76 \pm 0.56 \pm 0.38) \times 10^{-5}$			$(8.92 \pm 0.84 \pm 0.65) \times 10^{-5}$		$(2.27 \pm 0.43 \pm 0.25) \times 10^{-5}$	
$\mathcal{B}$ (PDG) [2]	$(1.96 \pm 0.21) \times 10^{-3}$			$< 1.0 \times 10^{-4}$			$< 23 \times 10^{-5}$		$< 6.0 \times 10^{-5}$	

Table II. The systematic uncertainties (in %) in the branching fraction measurement.

Decay channel	$\chi_{c0} \to$		$\chi_{c2} \to$	
	$\eta'\eta'$	$\eta\eta'$	$\eta'\eta'$	$\eta\eta'$
$N_{\psi(3686)}$	0.6	0.6	0.6	0.6
Tracking	4.0	2.0	4.0	2.0
Photon efficiency	2.2	2.6	2.2	2.6
η reconstruction	0.7	1.3	0.7	1.3
η' mass window	1.0	1.7	1.0	1.7
Kinematic fit	0.7	1.0	0.6	1.7
$\chi_{c0,2}$ signal fitting	1.1	5.0	3.9	9.5
Intermediate state $\mathcal{B}$	3.8	3.1	4.4	3.8
Veto $\pi^+\pi^- J/\psi$	0.1	-	0.9	-
Veto $\psi(3686) \to \pi^0 + X$	0.2	1.0	2.1	0.2
Veto $J/\psi \to \gamma\eta'$	-	0.8	-	1.5
Total	6.3	7.3	8.0	11.2

VI. SUMMARY

In summary, based on 448.1×10^6 $\psi(3686)$ events collected with the BESIII detector, the decays $\chi_{c2} \to \eta'\eta'$, $\chi_{c0} \to \eta\eta'$ and $\chi_{c2} \to \eta\eta'$ are observed for the first time with significances of 9.6σ, 13.4σ and 7.5σ, respectively, and the corresponding branching fractions are measured. The branching fraction of the decay $\chi_{c0} \to \eta'\eta'$ is also measured with improved precision. Table I summarizes the measured branching fractions of $\chi_{c0,2} \to \eta'\eta'$ and $\eta\eta'$. With the measured branching fractions, the relative strength r between the DOZI and SOZI violating amplitudes for the χ_{c0} and χ_{c2} decays to PP final states, is estimated to be around -0.15 according to Eq. (15) in Ref. [3] with its input parameters. This implies that the contribution from the DOZI violating amplitude is suppressed in $\chi_{c0,2} \to PP$ decays in comparison with the SOZI ones [3, 4]. In addition, we find $\mathcal{B}(\chi_{c0} \to \eta'\eta')/\mathcal{B}(\chi_{c2} \to \eta'\eta') \approx 45$, which is about one order larger than the ratios for other pseudoscalar meson pairs, ranging from 3 to 6 for $\pi^+\pi^-$, $\pi^0\pi^0$, K^+K^-, $K^0_S K^0_S$, $\eta\eta$ [2] and $\eta\eta'$. This large ratio is expected by the model proposed in Ref. [3] given a relatively suppressed DOZI-violating contribution. This may initiate further studies about the dynamics of $\chi_{c0,2} \to PP$.

The BESIII collaboration thanks the staff of BEPCII and the IHEP computing center for their strong support. This work is supported in part by the National Key Basic Research Program of China under Contract No. 2015CB856700; National Natural Science Foundation of China (NSFC) under Contracts Nos. 11575077, 11475090, 11475207, 11605042, 11235011, 11322544, 11335008, 11425524, 11305090, 11235005, 11275266; The China Scholarship Council; The Innovation Group of Nuclear and Particle Physics in USC; the Chinese Academy of Sciences (CAS) Large-Scale Scientific Facility Program; the CAS Center for Excellence in Particle Physics (CCEPP); the Collaborative Innovation Center for Particles and Interactions (CICPI); Joint Large-Scale Scientific Facility Funds of the NSFC and CAS under Contracts Nos. U1232201, U1332201, U1532257, U1532258; CAS under Contracts Nos. KJCX2-YW-N29, KJCX2-YW-N45; 100 Talents Program of CAS; National 1000 Talents Program of China; INPAC and Shanghai Key Laboratory for Particle Physics and Cosmology; German Research Foundation DFG under Contracts Nos. Collaborative Research Center CRC 1044, FOR 2359; Istituto Nazionale di Fisica Nucleare, Italy; Koninklijke Nederlandse Akademie van Wetenschappen (KNAW) under Contract No. 530-4CDP03; Ministry of Development of Turkey under Contract No. DPT2006K-120470; National Science and Technology fund; The Swedish Resarch Council; U. S. Department of Energy under Contracts Nos. DE-FG02-05ER41374, DE-SC-0010504, DE-SC0012069; University of Groningen (RuG) and the Helmholtzzentrum für Schwerionenforschung GmbH (GSI), Darmstadt; WCU Program of National Research Foundation of Korea under Contract No. R32-2008-000-10155-0

[1] Q. Zhao, B. S. Zou and Z. B. Ma, Phys. Lett. B **631**, 22 (2005).

[2] C. Patrignani *et al.* (Particle Data Group), Chin. Phys.

C **40**, 100001 (2016).
[3] Q. Zhao, Phys. Rev. D **72**, 074001 (2005).
[4] Q. Zhao, Phys. Lett. B **659**, 221 (2008).
[5] M. Ablikim *et al.* (BES Collaboration), Phys. Rev. D **70**, 092002 (2004); Phys. Rev. D **72**, 092002 (2005).
[6] M. Ablikim *et al.* (BESIII Collaboration), Phys. Rev. Lett. **107**, 092001 (2011).
[7] M. Ablikim *et al.* (BES Collaboration), Chin. Phys. C **37**, 063001 (2013).
[8] The total number of $\psi(3686)$ events taken at 2009 and 2012 is obtained based on the same method in Ref. [7]. The preliminary number is determined to be 448.1×10^6 with uncertainties of 0.7%.
[9] M. Ablikim *et al.* (BES Collaboration), Nucl. Instrum. Meth. A **614**, 345 (2010).
[10] S. Agostinelli *et al.* (GEANT4 Collaboration), Nucl. Instrum. Meth. A **506**, 250 (2003); J. Allison *et al.*, IEEE Trans. Nucl. Sci. **53**, 270 (2006).
[11] Z. Y. Deng *et al.*, High Energy Physics & Nuclear Physics **30**, 371 (2006).
[12] S. Jadach, B. F. L. Ward, and Z. Was, Comput. Phys. Commun. **130**, 260 (2000); Phys. Rev. D **63**, 113009 (2001).
[13] R. G. Ping, Chin. Phys. C **32**, 599 (2008); D. J. Lange, Nucl. Instr. Meth. A **462**, 152 (2001).
[14] J. C. Chen, G. S. Huang, X. R. Qi, D.H. Zhang, Y.S. Zhu, Phys. Rev. D **62**, 034003 (2000); R. L. Yang, R. G. Rong, D. Chen, Chin. Phys. Lett. **31**, 061301 (2014).
[15] E. Eichten, K. Gottfried, T. Kinoshita, K.D. Lane, T.M. Yan, Phys. Rev. D **21**, 203 (1980).
[16] M. Ablikim *et al.* (BESIII Collaboration), Phys. Rev. D **84**, 092006 (2011).
[17] M. Ablikim *et al.* (BESIII Collaboration), Chin. Phys. C **37**, 123001 (2013).
[18] M. Ablikim *et al.* (BESIII Collaboration), Phys. Rev. D **81**, 052005 (2010).
[19] M. Ablikim *et al.* (BESIII Collaboration), Chin. Phys. C **41**, 013001 (2017).
[20] M. Ablikim *et al.* (BESIII Collaboration), Phys. Rev. Lett. **105**, 261801 (2010).
[21] M. Ablikim *et al.* (BESIII Collaboration), Phys. Rev. D **87**, 012002 (2013).